Gyrokinetic Simulations of Solar Wind Turbulence and Magnetic Reconnection

Jason M. TenBarge
Collaborators: Greg Howes, Kris Kline, Bill Daughton, Homa Karimabadi

April 11, 2013

The University of Iowa

Outline

Why is turbulence important?

Turbulence is important because it governs the transport of

- Energy (energy flow, heating)
- Mass (mixing, accretion)
- Momentum (jet interactions, shocks)

Turbulence plays an important role in a large variety of space and astrophysical phenomena, e.g.,

- Accretion discs
- Interstellar medium
- Star-forming nebulae
- Solar corona and solar wind

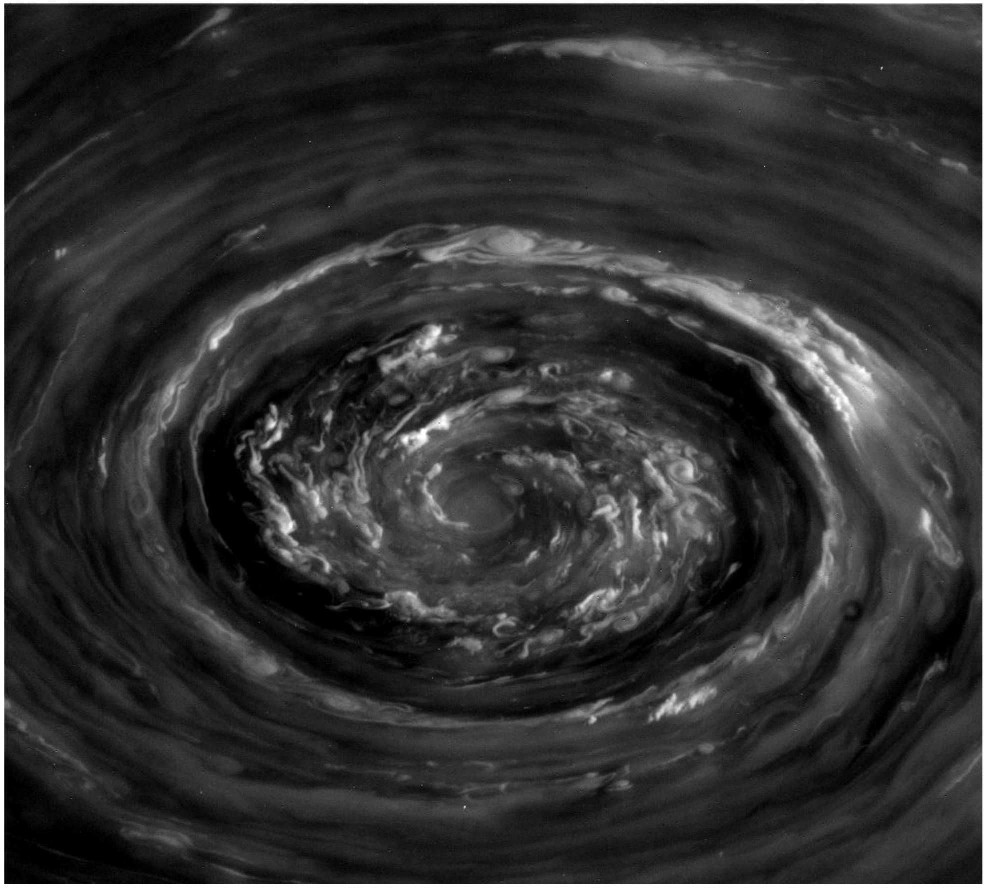

Alfvénic Turbulence

- Turbulence is mediated by interacting Alfvén waves
- In a magnetized plasma, large-scale magnetic field adds a preferential direction to the system
- Turbulence becomes anisotropic

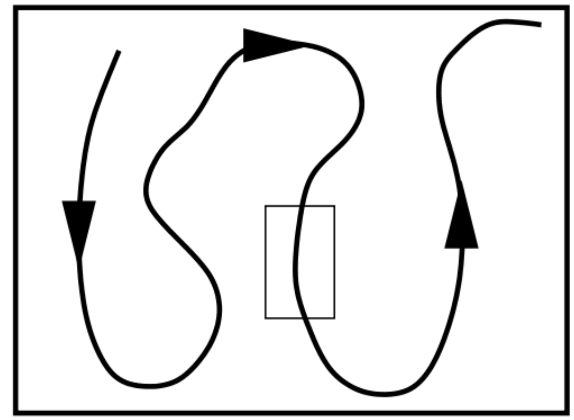

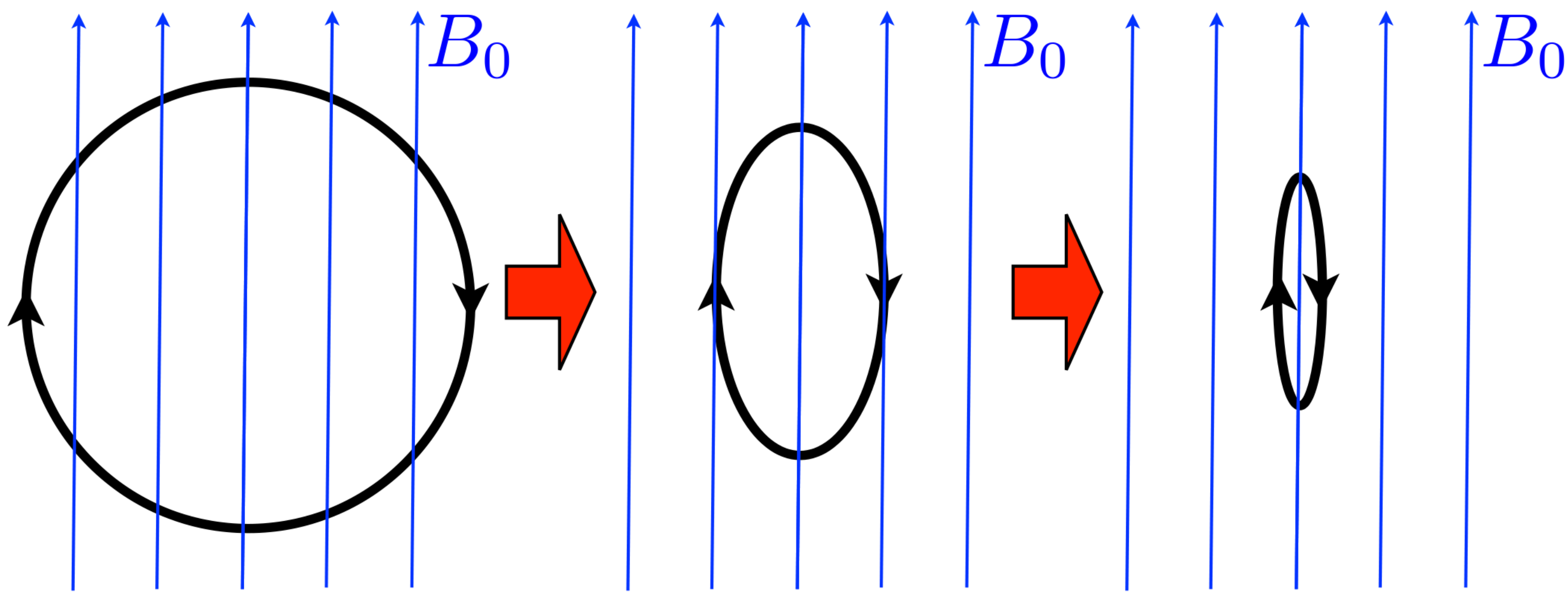

Gyrokinetics

What is gyrokinetics?

- Average quantities over the gyro-motion of particles and describe the evolution of rings rather than particles
- Gyro-averaged and ordered version of full Vlasov-Maxwell kinetic theory
- Basic ordering parameters: $\epsilon = \rho_i / a_0 \sim \delta f / F_0 \sim \omega / \Omega_i \sim k_{||} / k_\perp \ll 1$

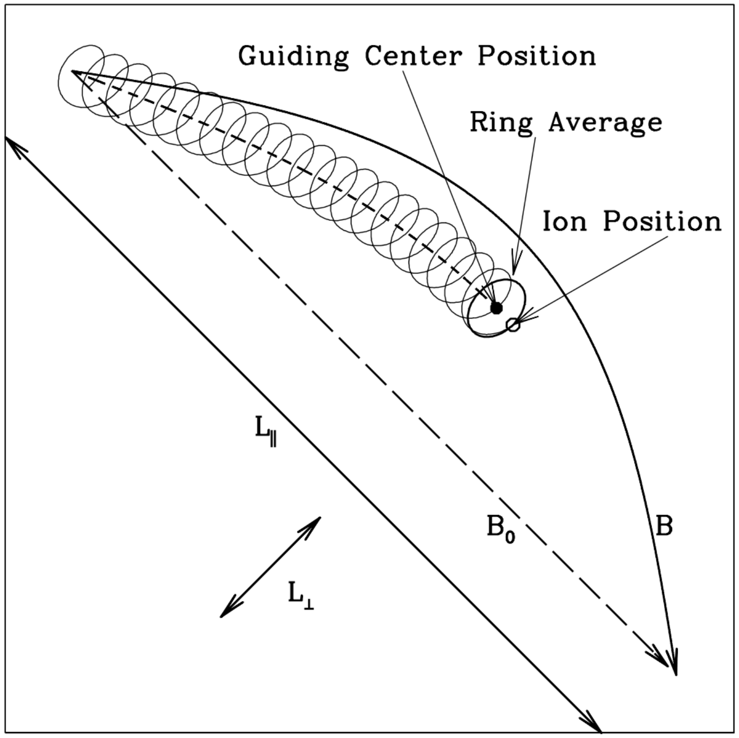

Why is it useful?

- Removes high frequency ($> \Omega_i$) fluctuations and reduces the problem from 6 to 5 dimensions
- Retains non-linear physics and kinetic effects (FLR, Landau damping, collisions)
- Ordering is concomitant to studies of turbulence

Solar Wind Energy Spectrum

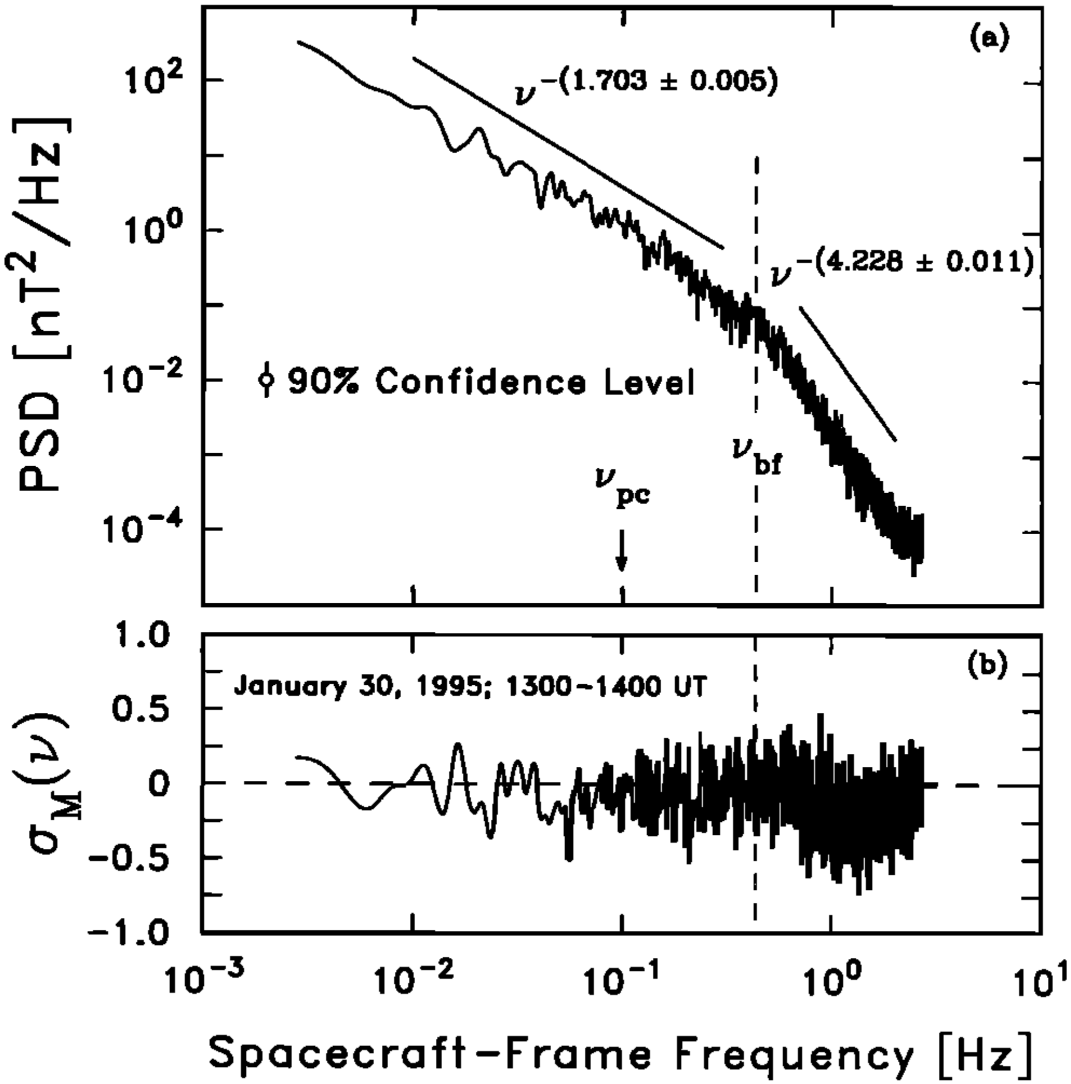

Magnetic energy spectrum (a) and magnetic helicity (b) from Leamon et al. [1998].

- Alfvénic inertial range transitions into something else at the spectral break
- Proposed to be kinetic Alfvén waves, magnetosonic whistler waves, ion cyclotron waves, or current sheets

More Recent Energy Spectra

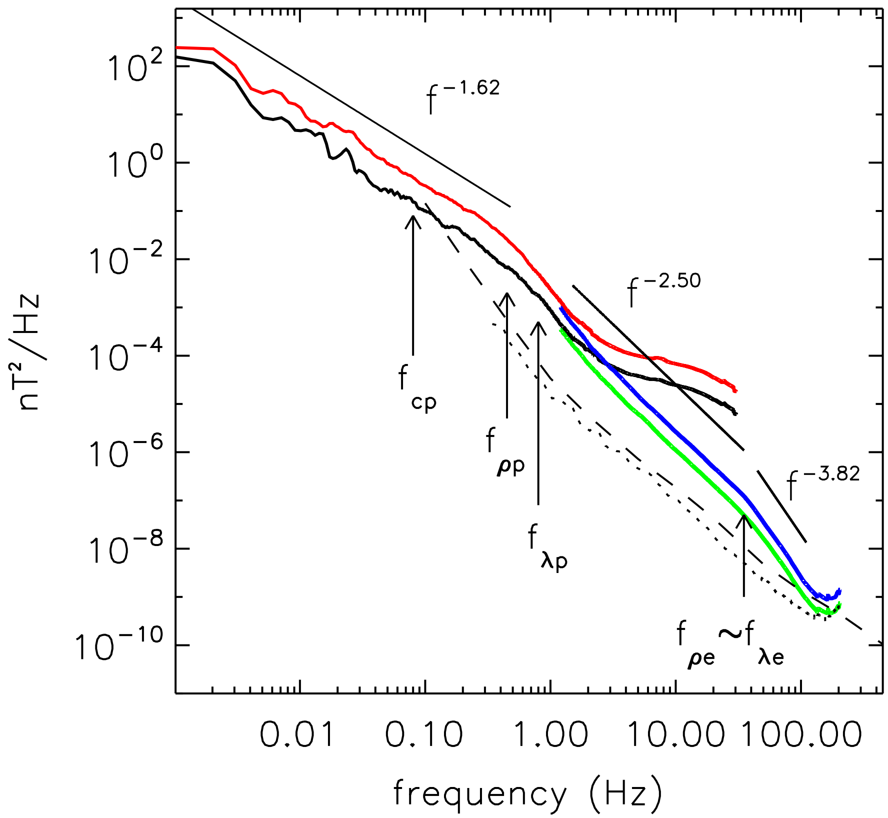

Magnetic energy spectrum from Sahraoui et al. [2009].

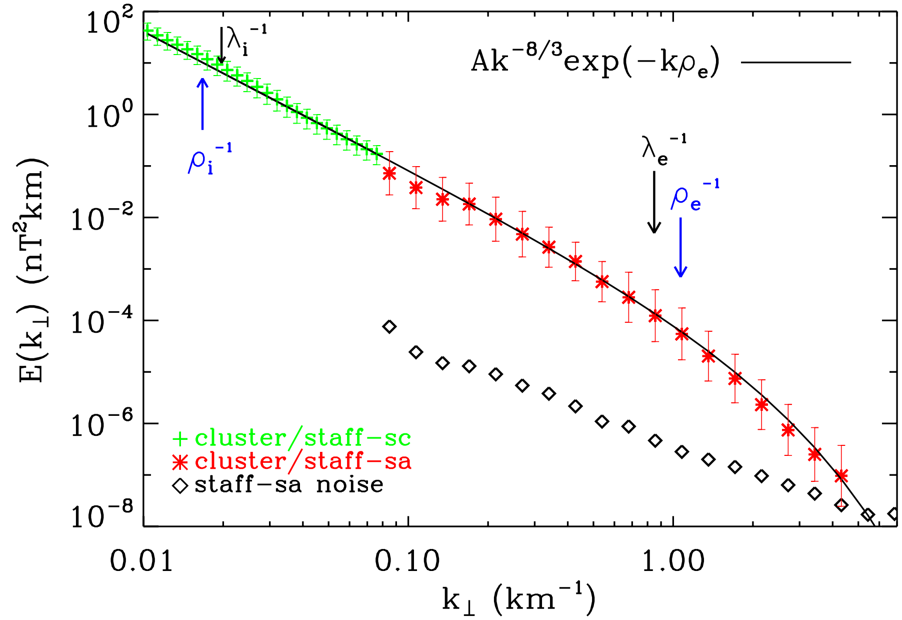

Average of 100 magnetic energy spectra from Alexandrova et al. [2012].

Evidence of KAWs (Support for Gyrokinetics)

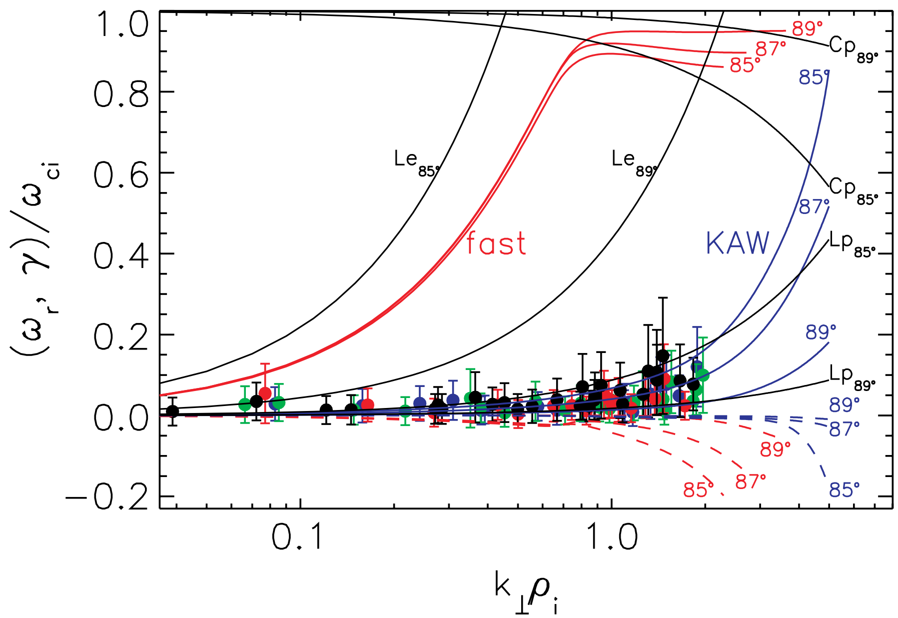

In situ solar wind dispersion relation from Sahraoui et al. [2010].

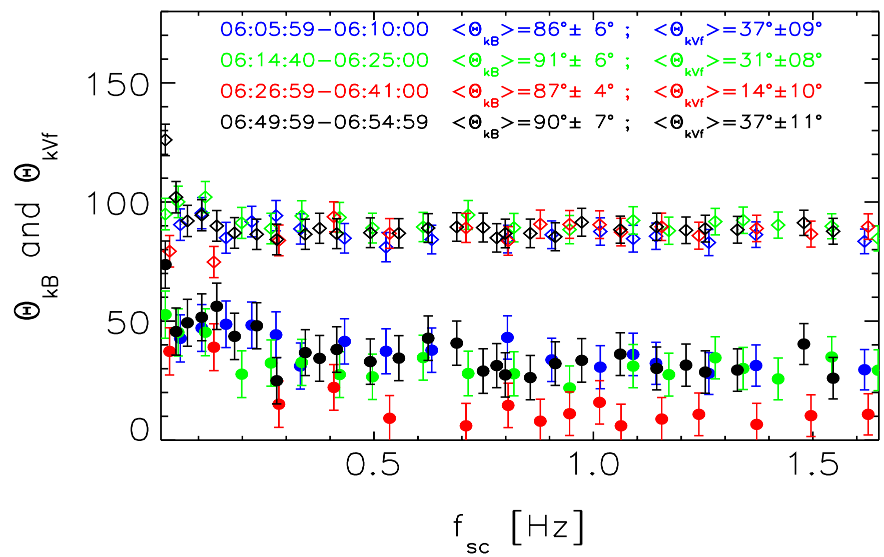

Angle between $\boldsymbol{k}$ and $\boldsymbol{B}$ Sahraoui et al. [2010].

Also observed by Roberts et al. [2013] with two additional intervals.

(Almost) No Fast Modes

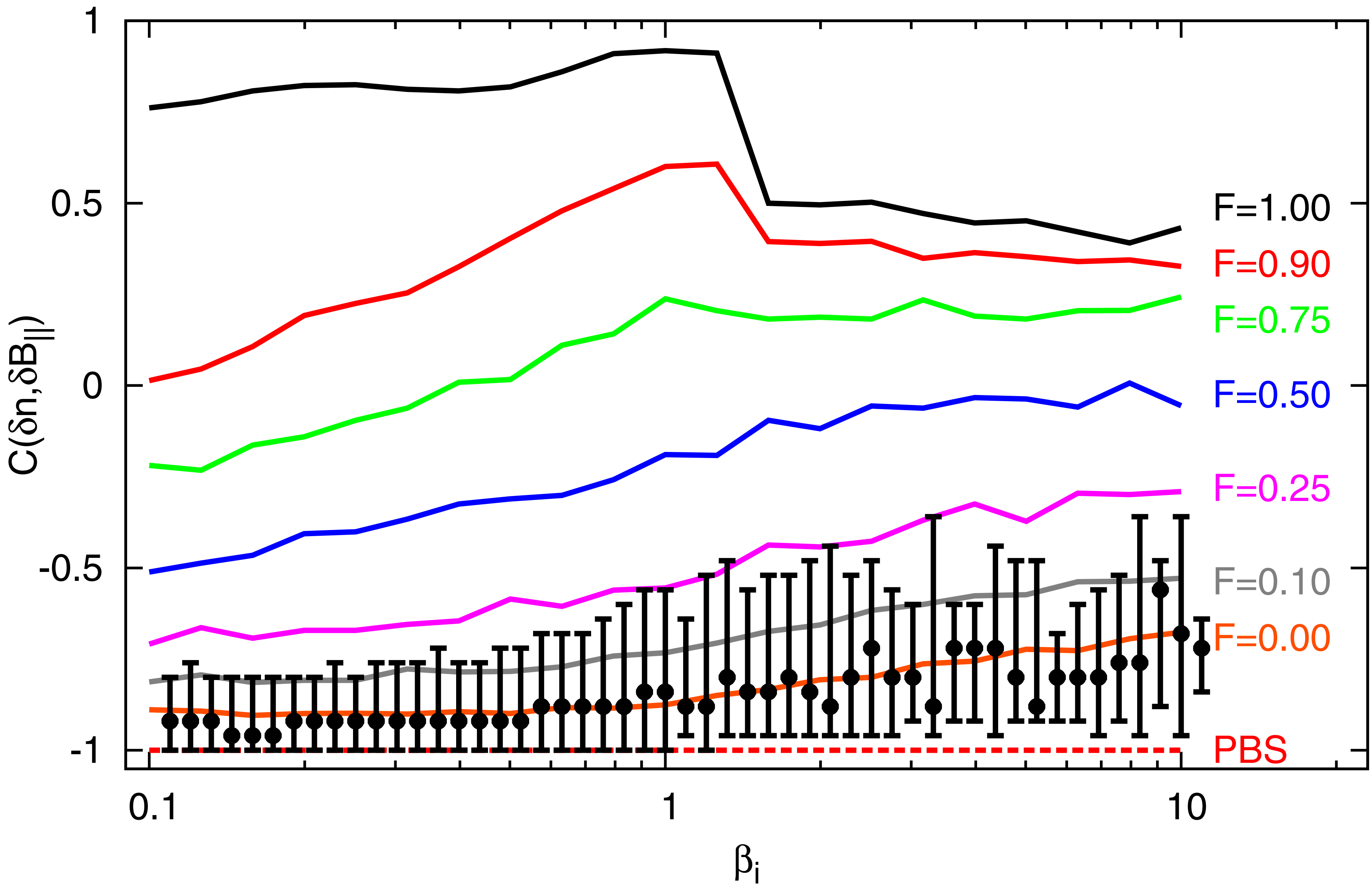

From Howes et al. [2012].

Particle Distributions

- Outer-scale $\sim 10^5 km$, $\lambda_{mfp} \sim 10^8 km$, $\rho_i \sim 100 km$
- Core (Maxwellian) distribution represents 95% of plasma
- Most probable $T_\perp / T_\parallel = 0.89$

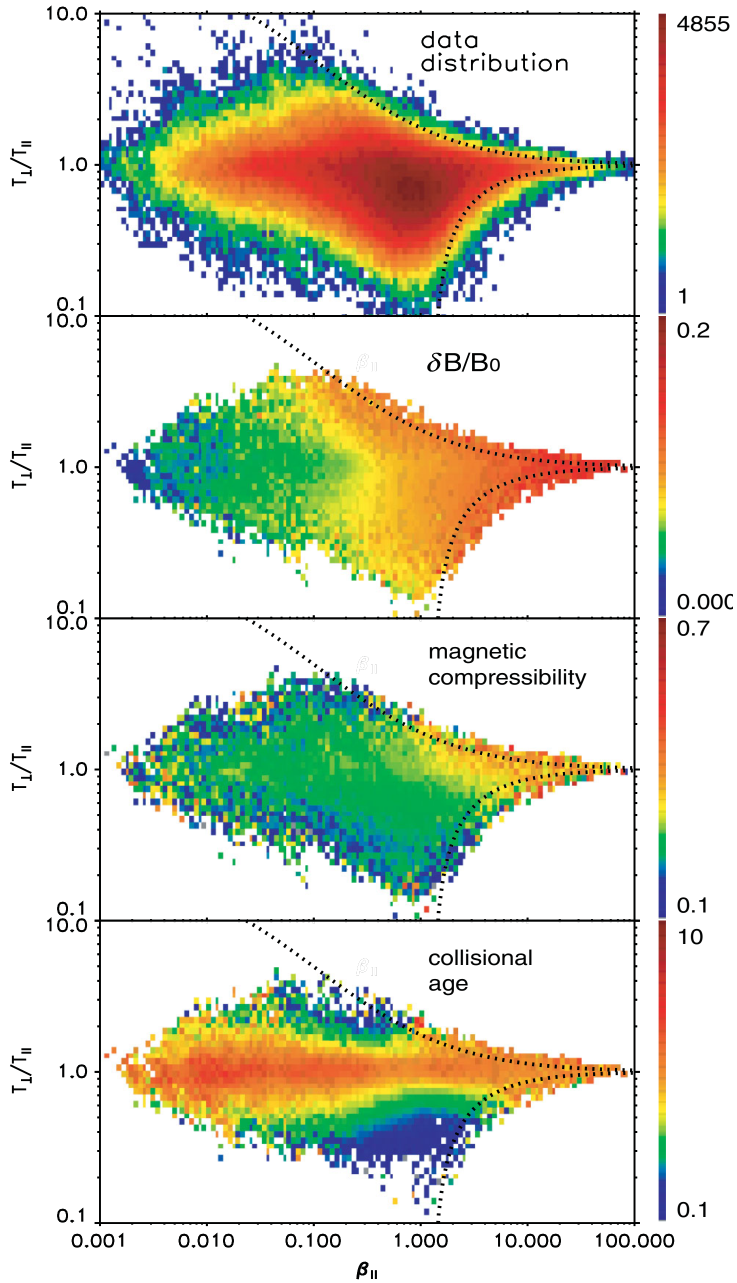

From Bale et al. [2009].

Turbulence at Kinetic Scales

- Anisotropic cascade of MHD Alfvén waves transitions to a cascade of kinetic Alfvén waves at the ion Larmor radius, ρ_i.
- Dissipation begins at ion kinetic scales in the form wave-particle interactions (Landau, transit-time, cyclotron, ...).
- Current sheets also form at ion scales and may be responsible for dissipation.
- Which mechanism is dominant in weakly collisional kinetic plasmas?

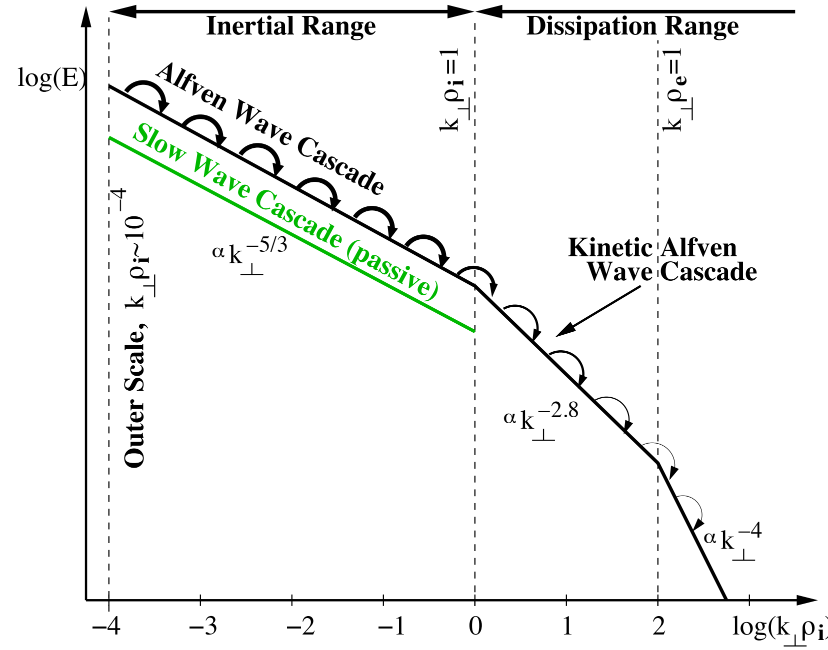

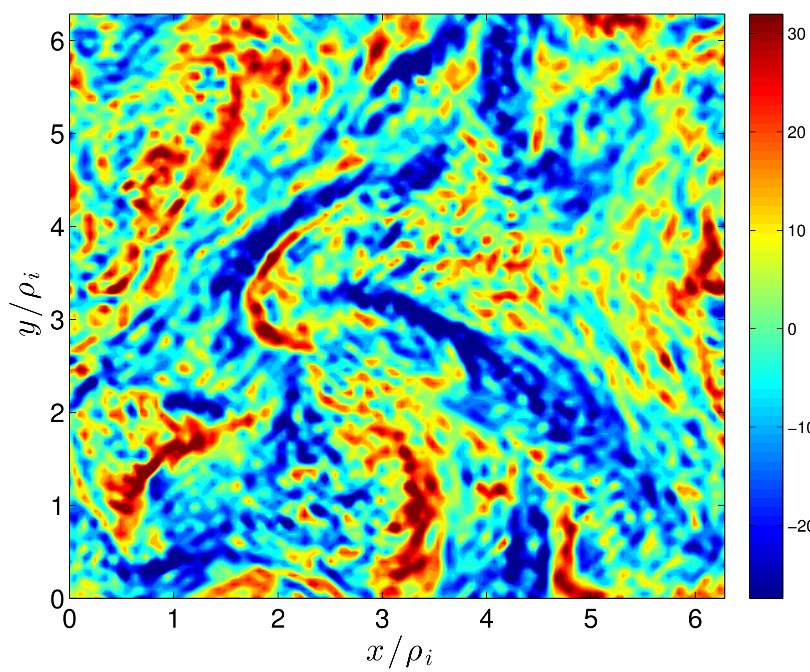

Turbulence at Kinetic Scales

- Anisotropic cascade of MHD Alfvén waves transitions to a cascade of kinetic Alfvén waves at the ion Larmor radius, ρ_i.
- Dissipation begins at ion kinetic scales in the form wave-particle interactions (Landau, transit-time, cyclotron, ...).
- Current sheets also form at ion scales and may be responsible for dissipation.
- Which mechanism is dominant in weakly collisional kinetic plasmas?

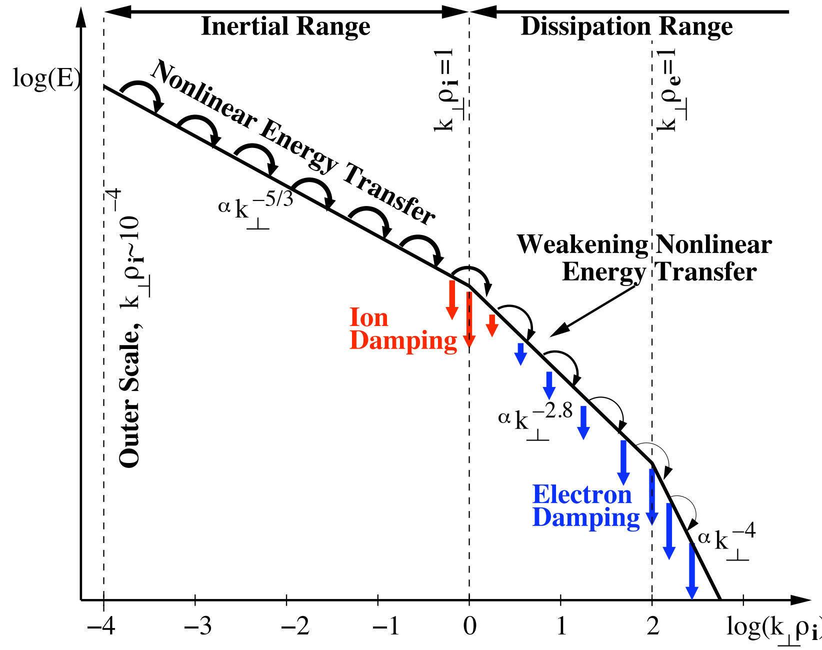

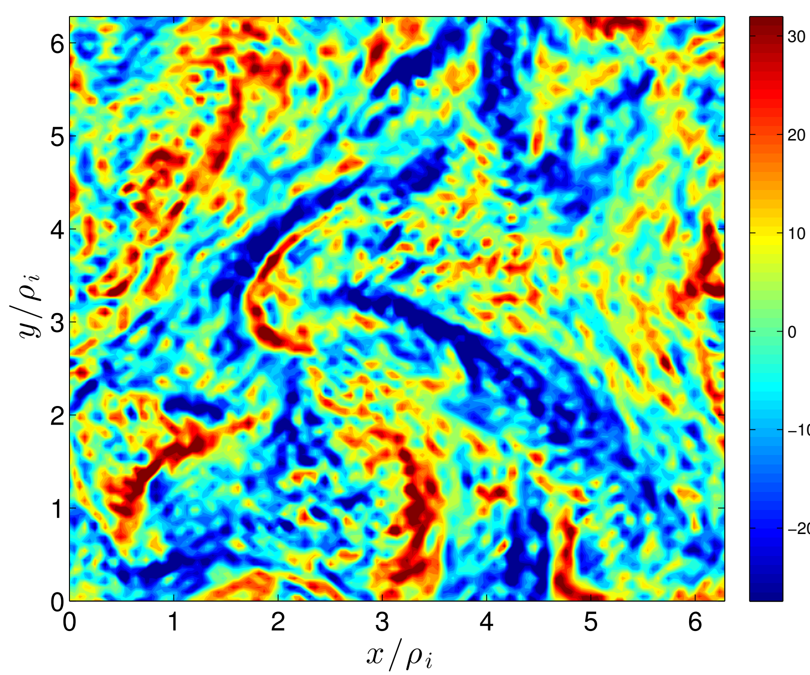

AstroGK

- Based on GS2, a mature fusion gyrokinetics code
- Eulerian initial-value code with periodic boundary conditions in slab geometry
- Evolves 5D phase space for each species
- Fully non-linear, with number, momentum, and energy conserving collision operator
- Realistic mass ratio, $\beta_p = 1$, $T_p = T_e$, weakly collisional ($\nu_s \ll \omega_{min}$)
- Driven at outer-scale with Langevin antenna current coupled to $A_\|$—injects Alfvén like waves at outer-scale

Why Antenna Driven?

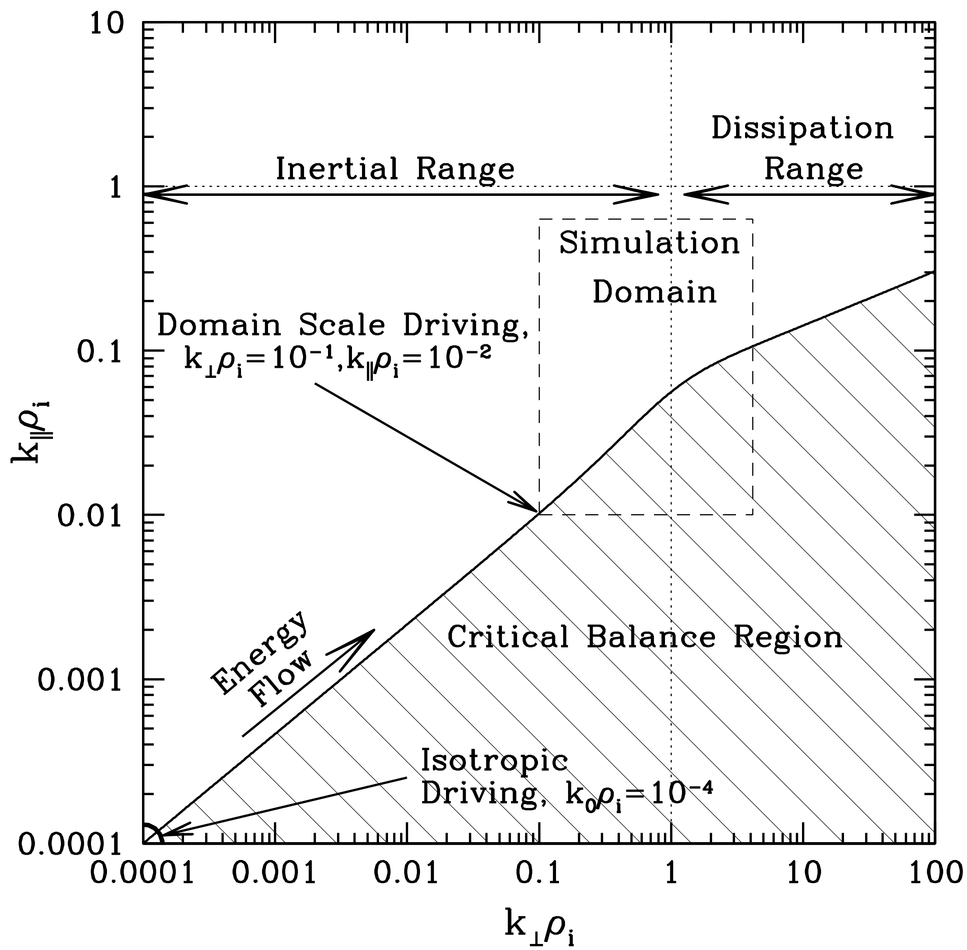

Schematic diagram of the distribution of energy in the $k_\perp - k_\parallel$ plane, highlighting the turbulence driving scale, typical simulation domain, and domain scale driving. From TenBarge et al. [2013b].

- Solar wind and astrophysical plasmas tend to be driven by external sources
- Finite and small simulation domain requires energy input consistent with cascade from larger scales
- Allows specification of central amplitude and frequency as well as decorrelation rate for chosen $\mathbf{k}$ vector

Why Langevin?

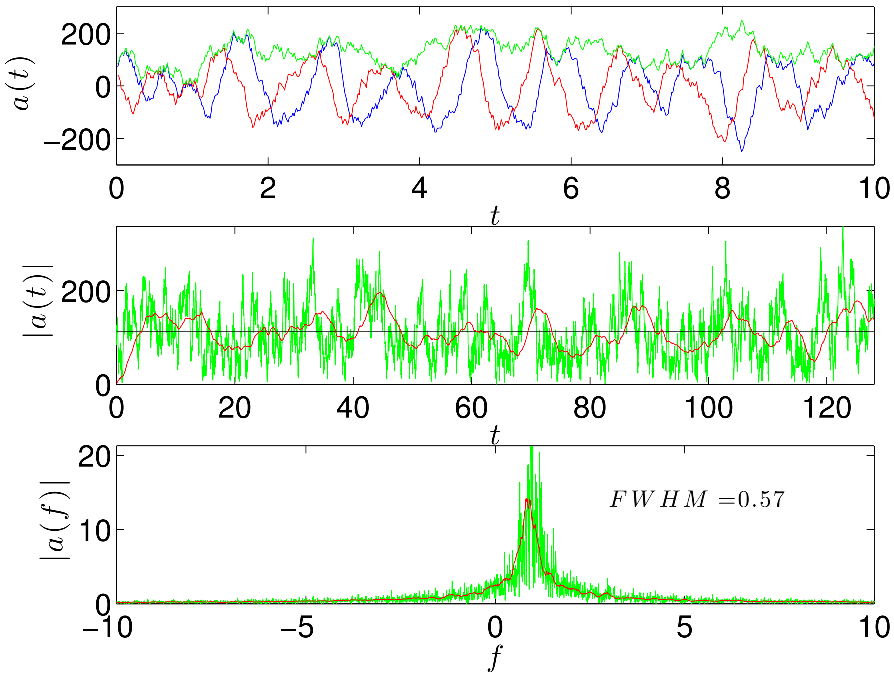

Example of a single oscillating Langevin antenna with $A_0 = 100$, $\omega_0 = 2\pi$ rad/s, and $\gamma_0 = -1$ rad/s. From TenBarge et al. [2013b].

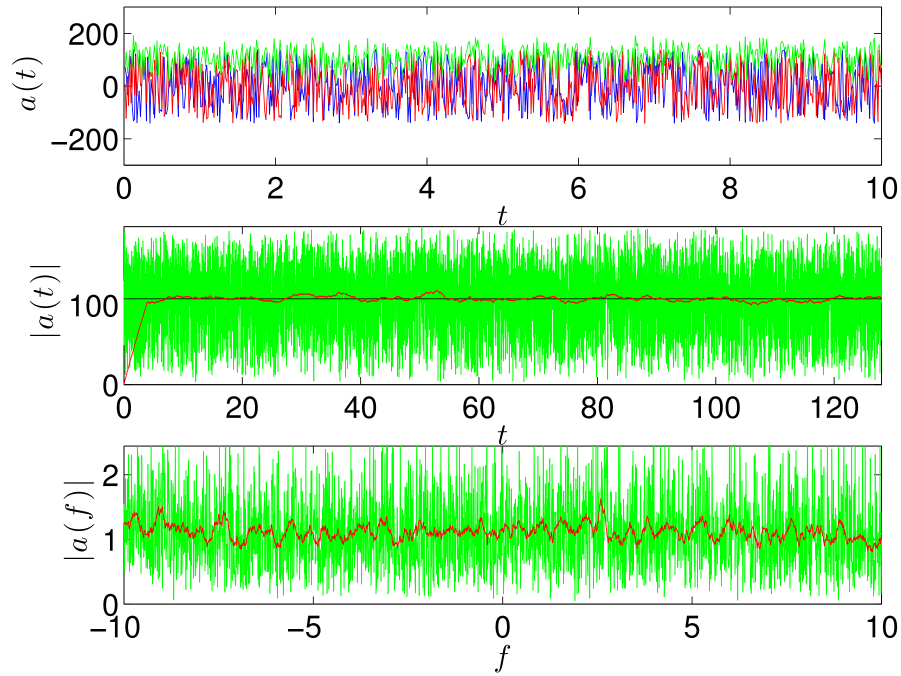

Example of a single delta-correlated white noise antenna with $A_0 = 100$. From TenBarge et al. [2013b].

Ion Scale Spectra

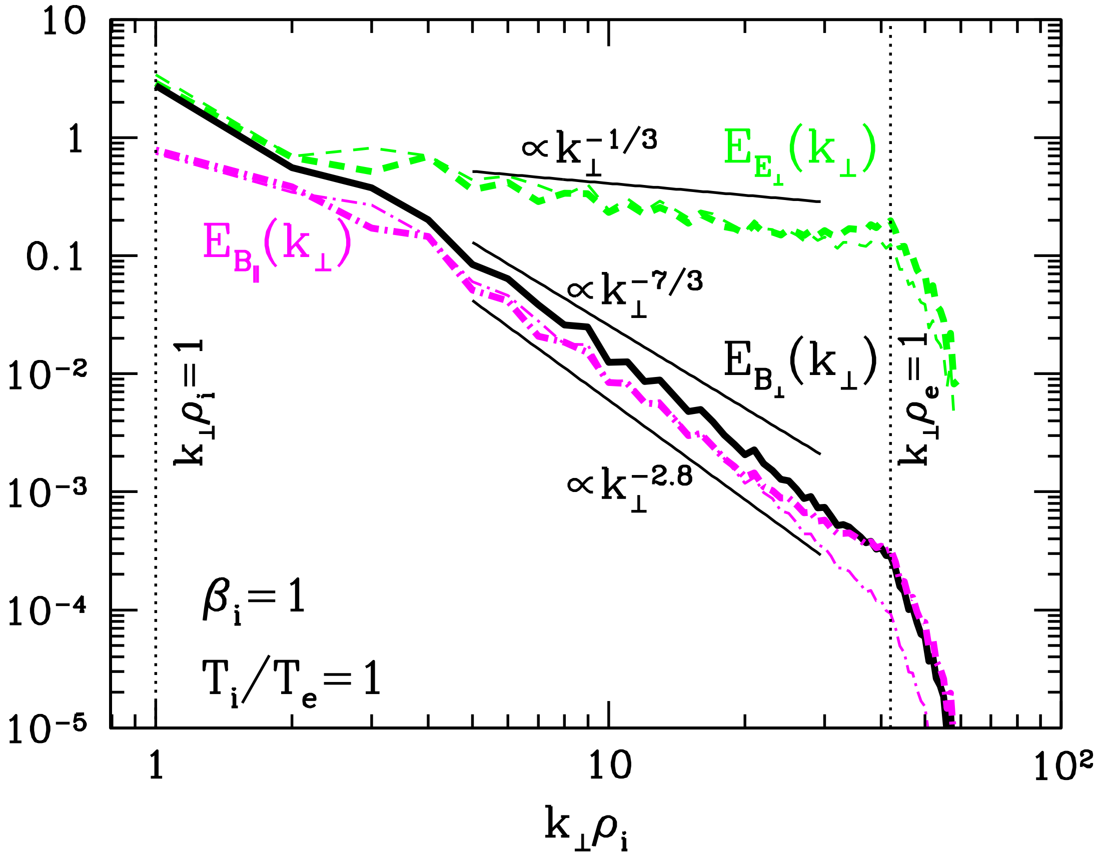

Energy spectra from AstroGK simulation from Howes et al. [2011b].

- Ion scale simulation, $k_\perp \rho_i \in [1, 42] \equiv k_\perp \rho_e \in [0.02, 1]$
- Spectrum agrees well with solar wind observations, e.g., Kiyani et al. [2009], Alexandrova et al. [2009], Sahraoui et al. [2010]
- Insufficient resolution to determine behaviour at electron scales

Electron Scale Spectra

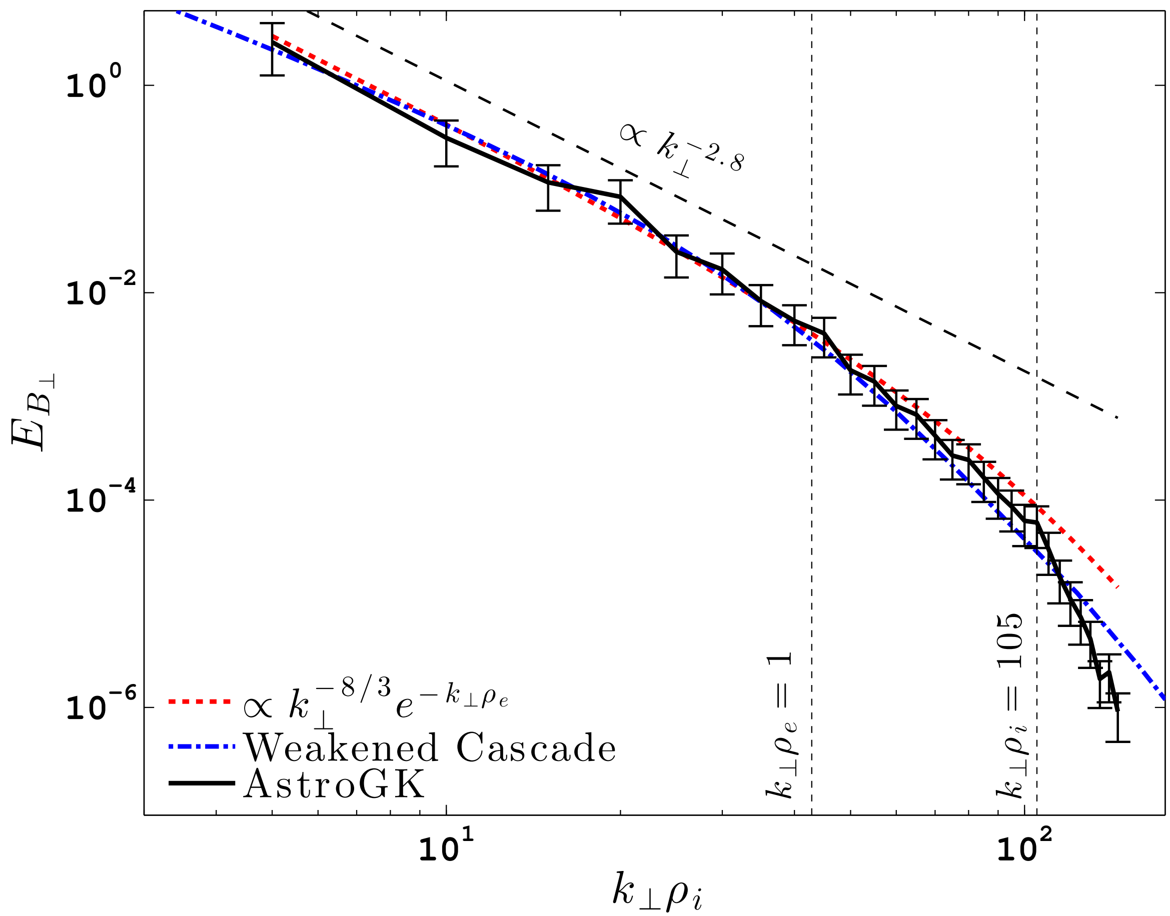

One dimensional magnetic energy spectra from AstroGK averaged over three turn-around times (solid black), weakened cascade model (blue dash-dotted), and the empirical form from Alexandrova et al. [2012] (red dotted).

- Electron scale simulation, $k_\perp \rho_i \in [5, 105] \equiv k_\perp \rho_e \in [0.12, 2.5]$
- Average spectrum agrees well with the exponential observed by Alexandrova et al. [2012].
- AstroGK spectrum also reproduced by weakened cascade model [Howes et al., 2011a].

Composite Spectrum

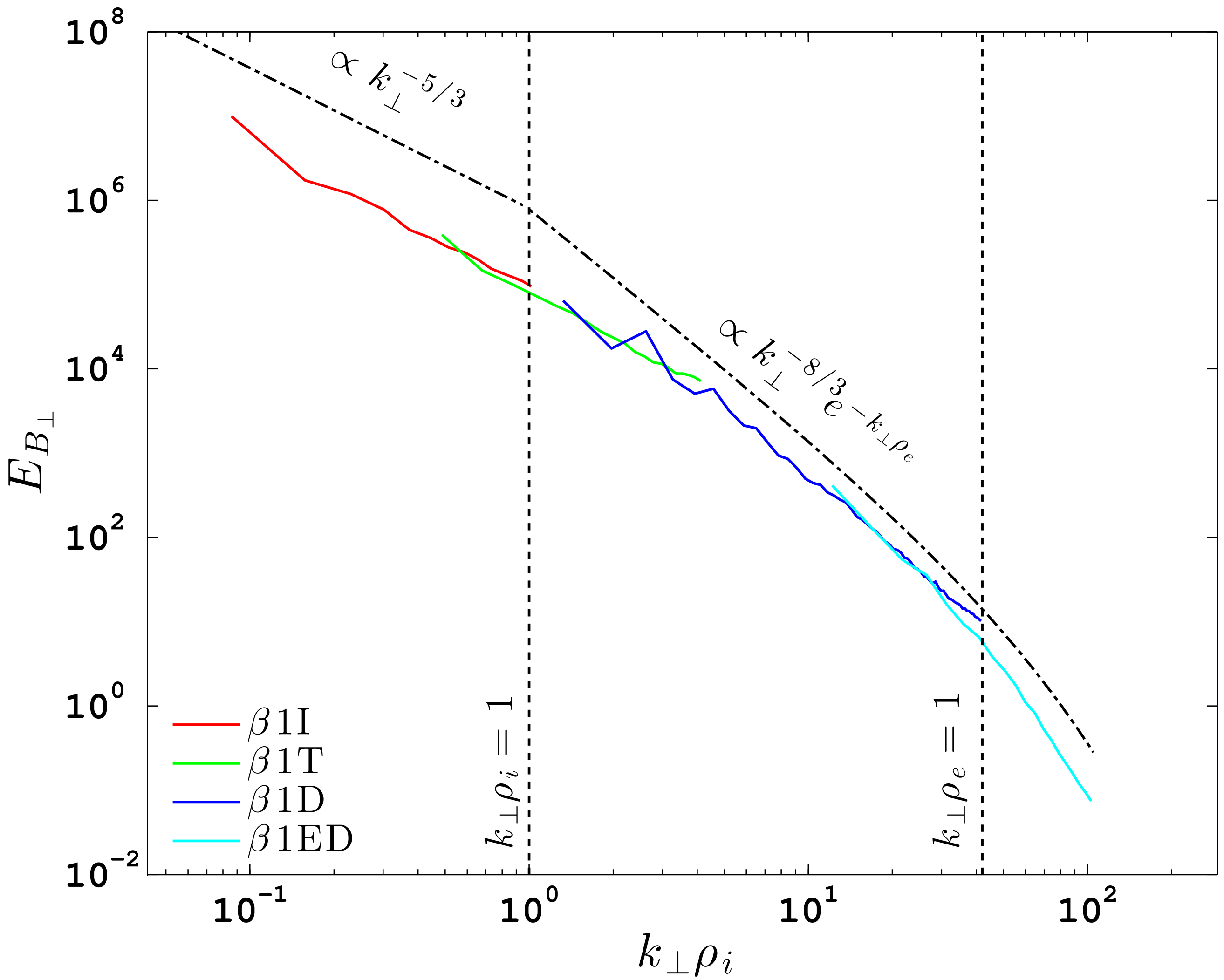

Composite spectrum of four AstroGK simulations with similar parameters spanning $k_\perp \rho_i \in [0.05, 105]$. From TenBarge et al. [2012].

Anisotropy at Kinetic Scales

Alfvénic turbulence is observed to obey two related properties

- Critical balance: $\chi = \frac{\omega_{nl}}{\omega_l} \simeq 1$
- Wavevector anisotropy: $k_\parallel \propto k_\perp^\xi$

The linear KAW frequency follows the general scaling with wavevector $\omega_l \propto k_\parallel k_\perp$. The frequency will therefore scale as $\omega_l \propto k_\perp^{\xi+1}$.

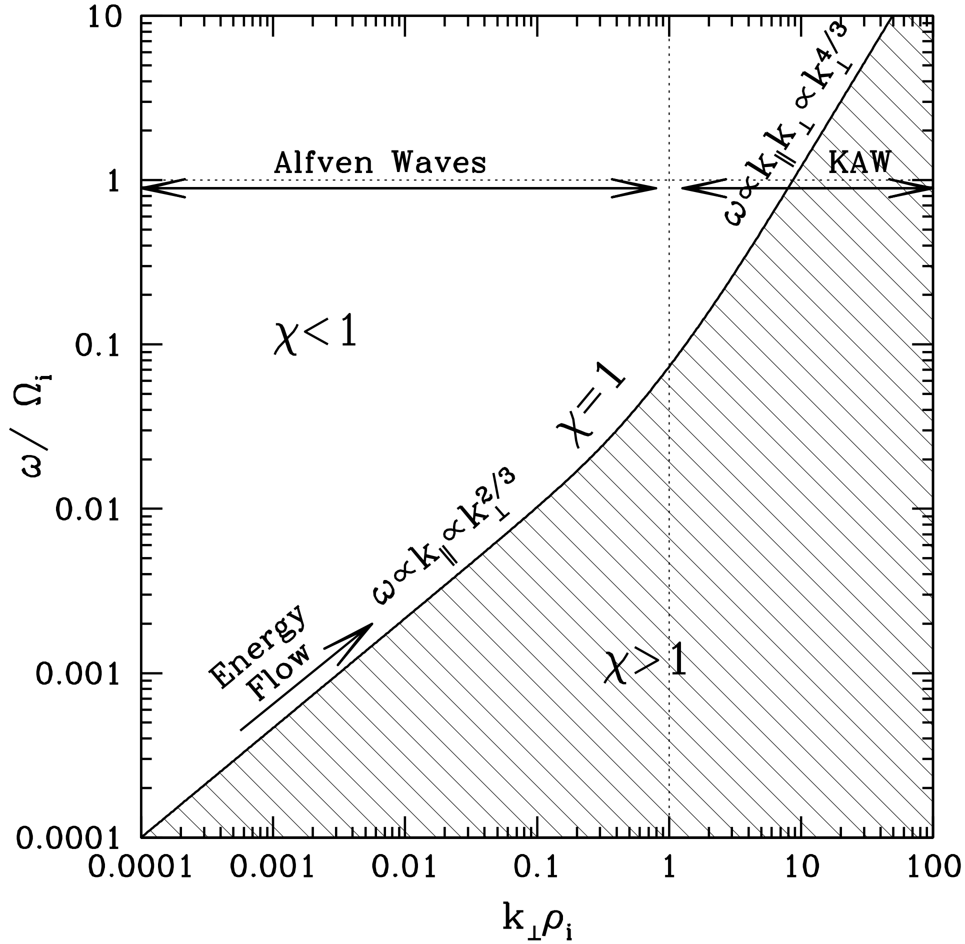

Schematic diagram of the energy distribution in the $k_\perp - \omega$ plane assuming critical balance holds. FromTenBarge and Howes [2012]

Evidence of Critical Balance

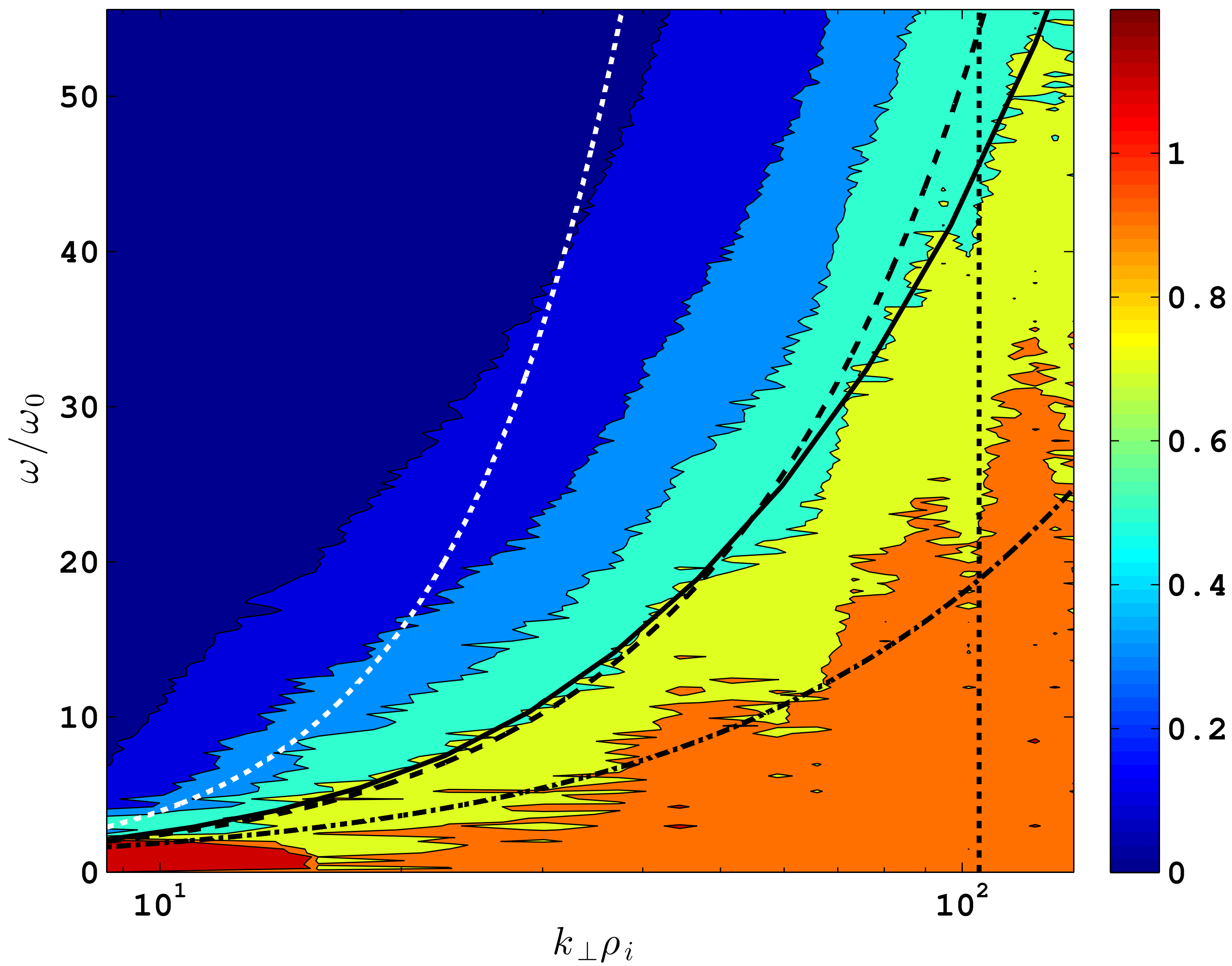

Contour plot of $E_{B_\perp}(\omega, k_\perp)/E_{B_\perp}(0, k_\perp)$ from an AstroGK simulation. Predictions for the envelope of the turbulent power are given for $\xi = 0$ (dot-dashed), $\xi = 1/3$ (dashed), $\xi = 1$ (dotted), and for the spectral anisotropy predicted by the weakened cascade model (solid). From TenBarge et al. [2013a].

Current Sheet Formation

- First wave-driven, 3D, kinetic study of current sheet evolution in turbulent plasma
- Current sheets form and persist for $\simeq 0.1 t_0$
- Strongest sheets correspond to field rotations approaching 180°
- Exist down to electron scales, below which no structure exists

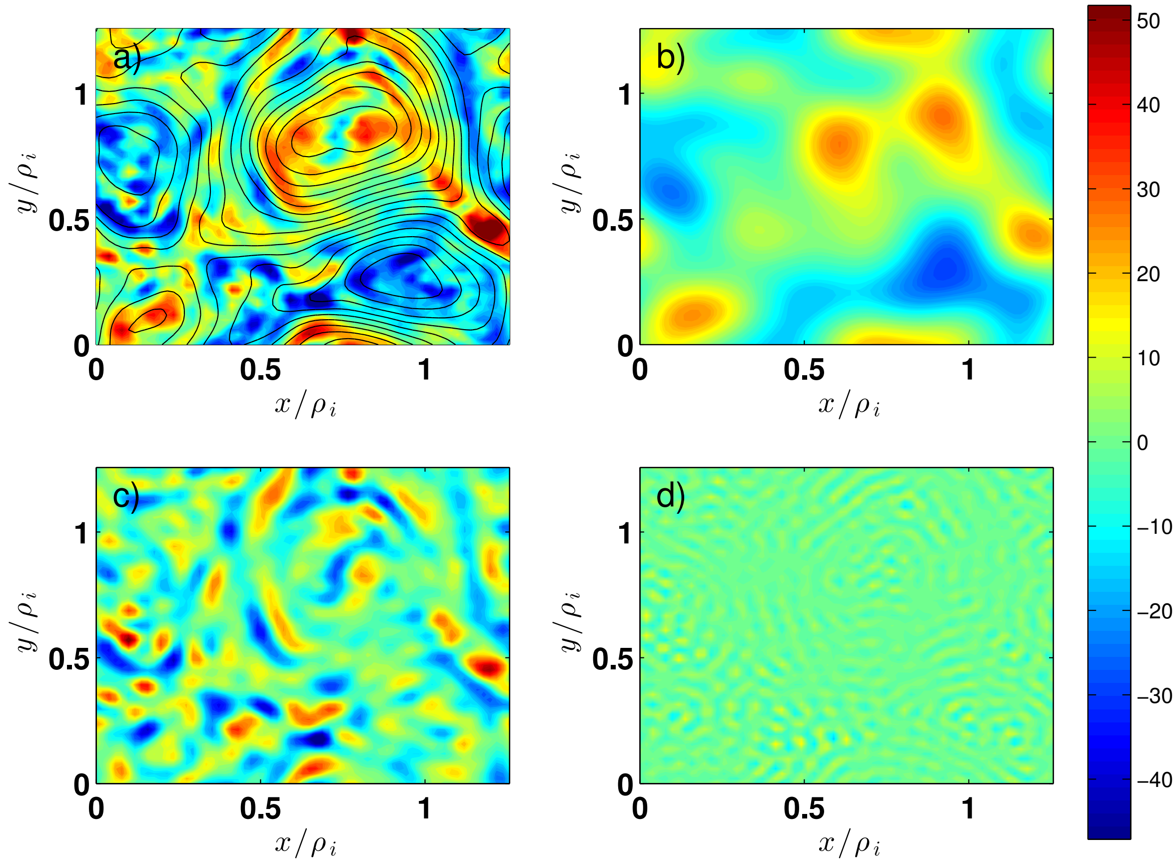

Parallel current density, j_z, for a perpendicular plane, with different band-pass filters applied: (a) unfiltered, (b) $5 \leq k_\perp \rho_i < 21$, (c) $21 \leq k_\perp \rho_i < 84$, and (d) $k_\perp \rho_i \geq 84$. Contours of the parallel vector potential A_z are shown in (a).

Electron Collisional Heating Rate

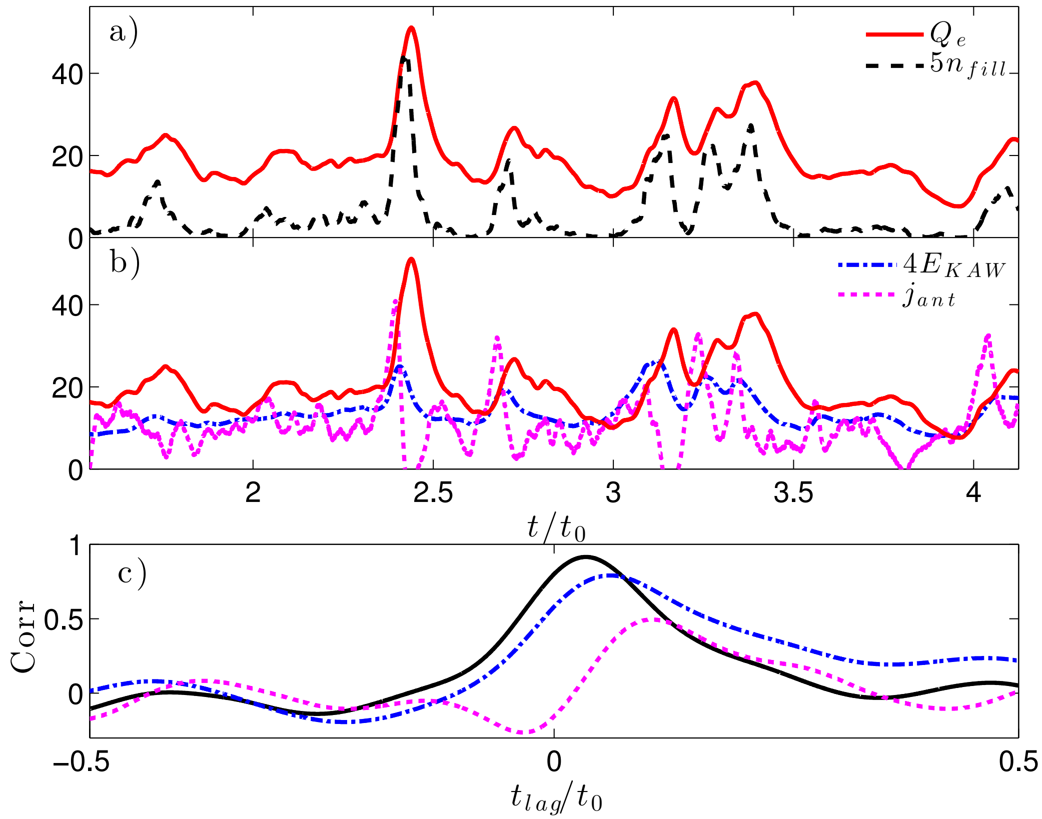

- Filling fraction is computed as the percentage of the volume with current density $j > j_{max}/3$.
- $E_{KAW} = E_B + E_{KE}$ is the total energy of the turbulent fluctuations in the simulation.
- Over six simulations: $\langle \max(\text{Corr}(Q, j_{ant})) \rangle = 0.52 \pm 0.02$ $\langle \max(\text{Corr}(Q, E_{KAW})) \rangle = 0.78 \pm 0.04$ $\langle \max(\text{Corr}(Q, n_{fill})) \rangle = 0.91 \pm 0.04$

Heating by k

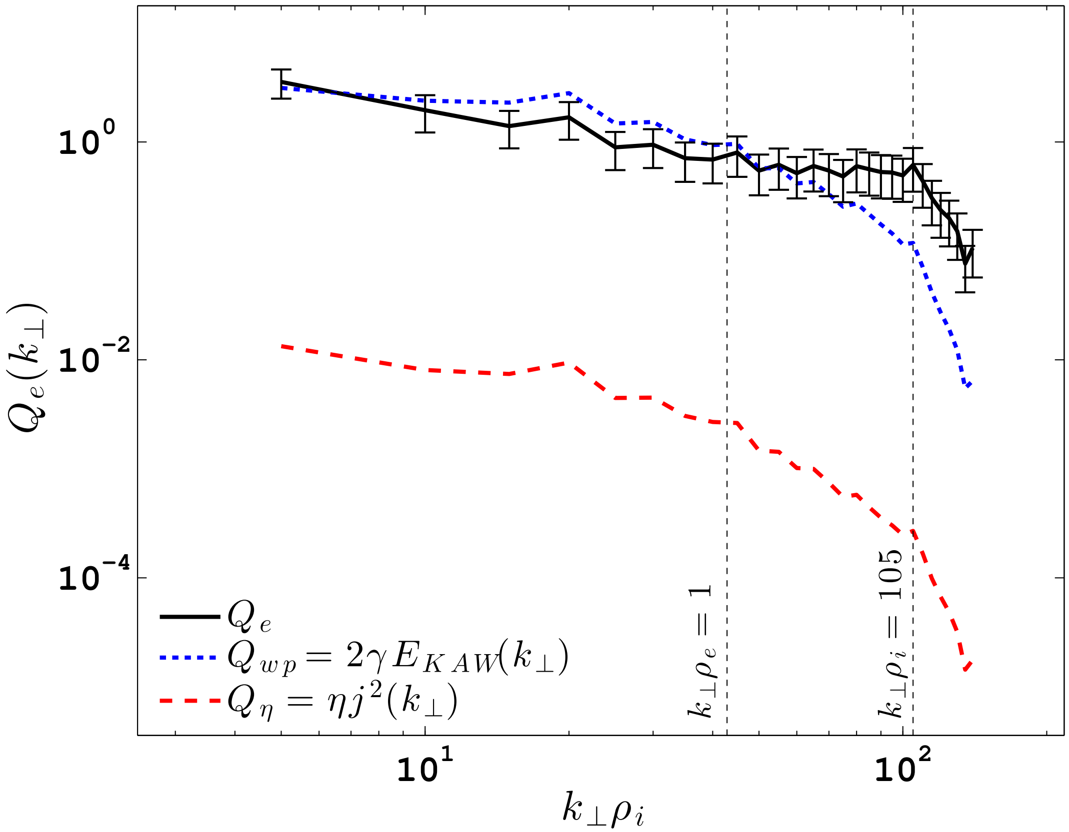

Total heating of the electrons from the simulation (solid black), an estimate of the electron heating based on linear wave-particle damping (dotted blue), and the Ohmic heating rate (dashed red).

- Resistive heating rate, ηj^2, calculated using Spitzer resistivity
- Integrated, total predicted electron heating (dotted blue) is within 4% of the collisional heating diagnosed in AstroGK (solid black)—no free parameters
- Slight disagreement by scale can be explained by electron entropy cascade

Discussion

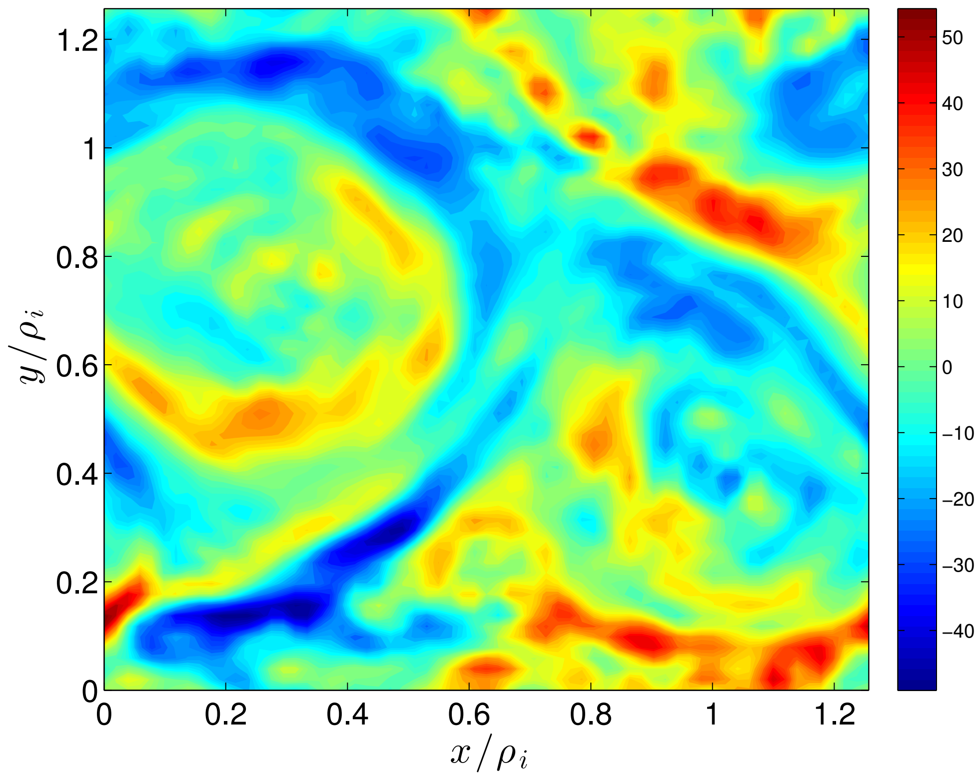

- Current sheets form as a natural consequence of turbulence
- They may be associated with dissipation, but that dissipation can take several forms: reconnection, resistive, or wave-particle.
- Wave-particle damping associated with current sheets requires they have parallel extent and propagation, which is absent in the majority of 2D studies of reconnection in turbulence.

PIC Reconnection Comparison

- To better understand the limitations of gyrokinetics on a detailed level, we have undertaken a direct comparison with PIC.
- PIC should converge to gyrokinetics in the correct asymptotic regime: $\delta B \ll B_g$ and small drift velocity $U_{ez} \ll v_{te}$.
- Parameters of the first set of simulations:
  $\beta_i = 8\pi n_{0i} T_{0i}/B_g^2 = 0.01$, $m_i/m_e = 1/25$, $T_{i0}/T_{e0} = 1$,
  $L_x = L_y = 20\pi\rho_i$, $a = 2\rho_i$, $n_x = n_y = 512$,
  $\delta B_{pert} = 0.02\delta B_{Harris}$.
- Periodic domain requires simulating double Harris-like sheet configuration.

Fully Kinetic PIC Simulations

Use a single Force-Free Harris sheet

$L = d_e$	$m_i/m_e = 25$	$v_{the}/c = 0.125$
$X_{max} = 15.7 d_e$	$n_x = 256$	
$Y_{max} = 31.4 d_e$	$n_y = 512$	$\beta_e = \beta_i = 0.01$

Hold these Fixed!

Consider 3 simulations that should approach GK orderings.
These correspond to a progressively weaker current sheet

Run1	$B_{zo} = 10 B_{yo}$	$\beta_{rx} = 1$	$\omega_{pe}/\Omega_{ce} = 8$	$U_{ez}/v_{the} = 1$
Run2	$B_{zo} = 20 B_{yo}$	$\beta_{rx} = 4$	$\omega_{pe}/\Omega_{ce} = 16$	$U_{ez}/v_{the} = 0.5$
Run3	$B_{zo} = 40 B_{yo}$	$\beta_{rx} = 16$	$\omega_{pe}/\Omega_{ce} = 32$	$U_{ez}/v_{the} = 0.25$

Based on reconnecting component

Peak electron fluid drift

PIC Reconnection First Results

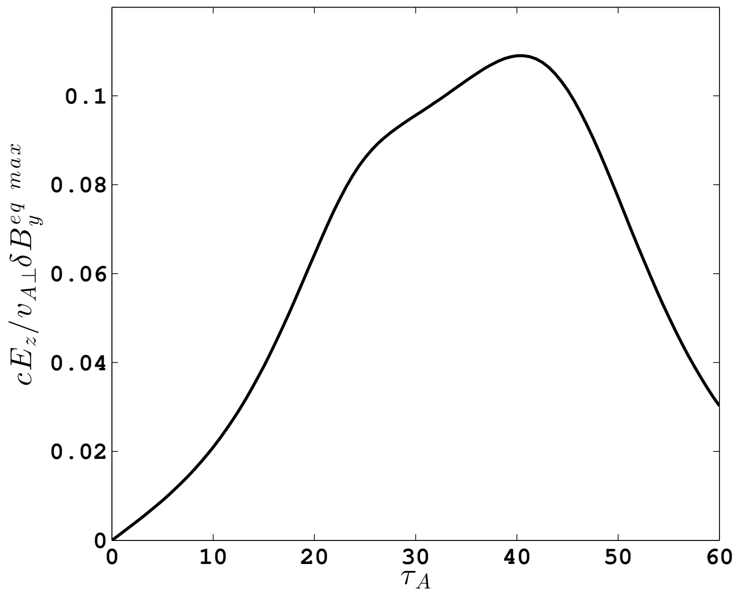

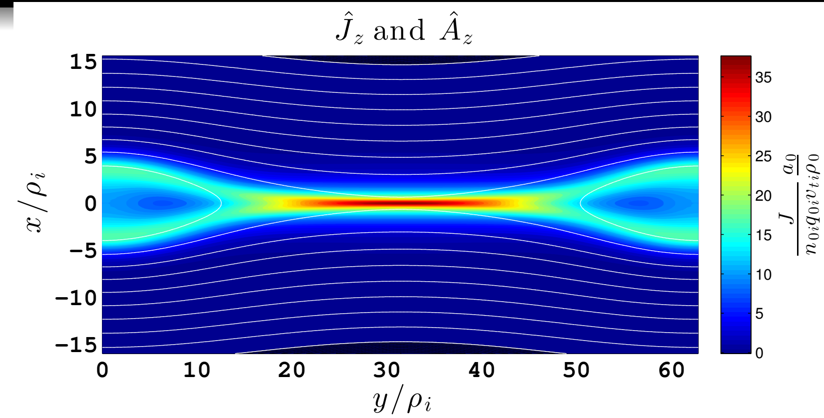

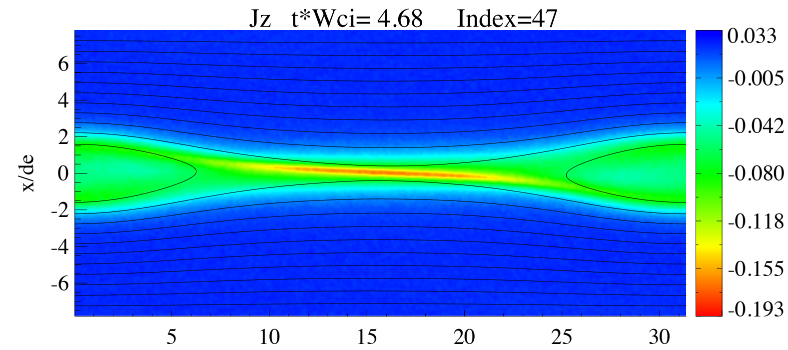

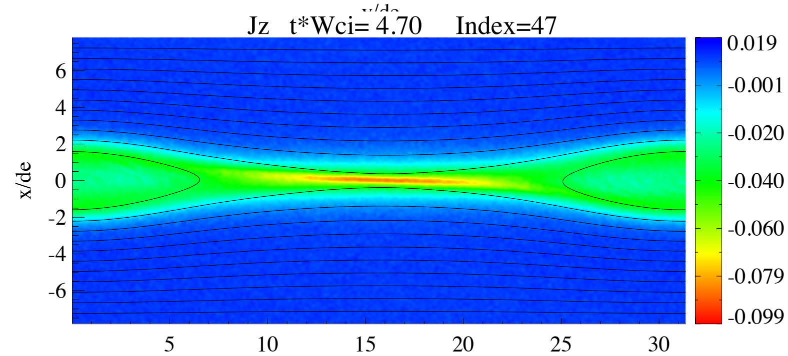

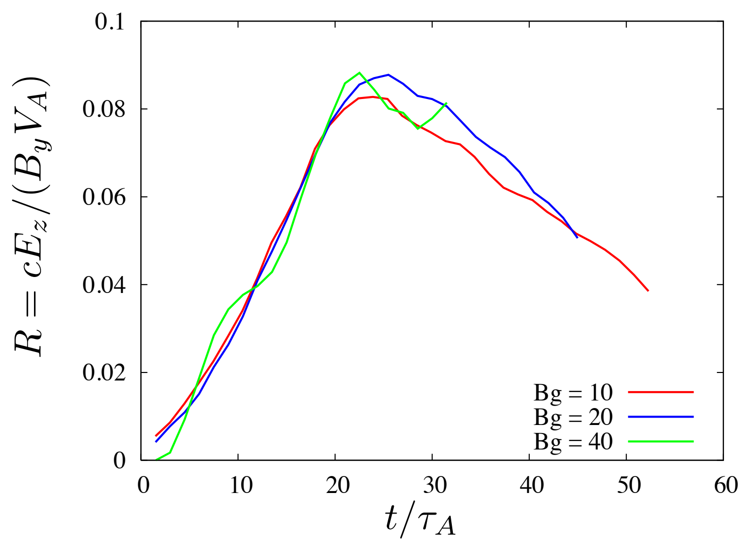

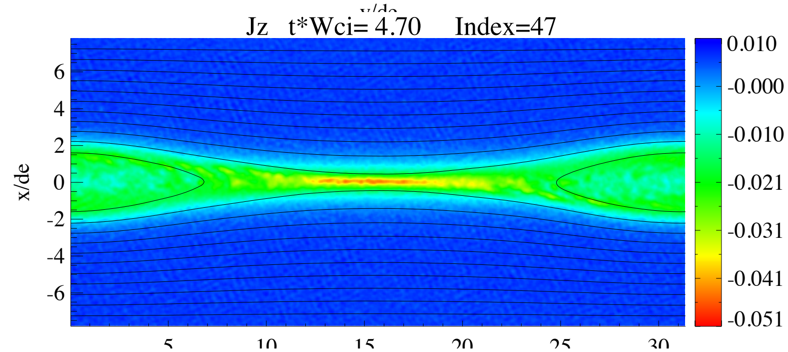

PIC Comparison δn_e and δB_z

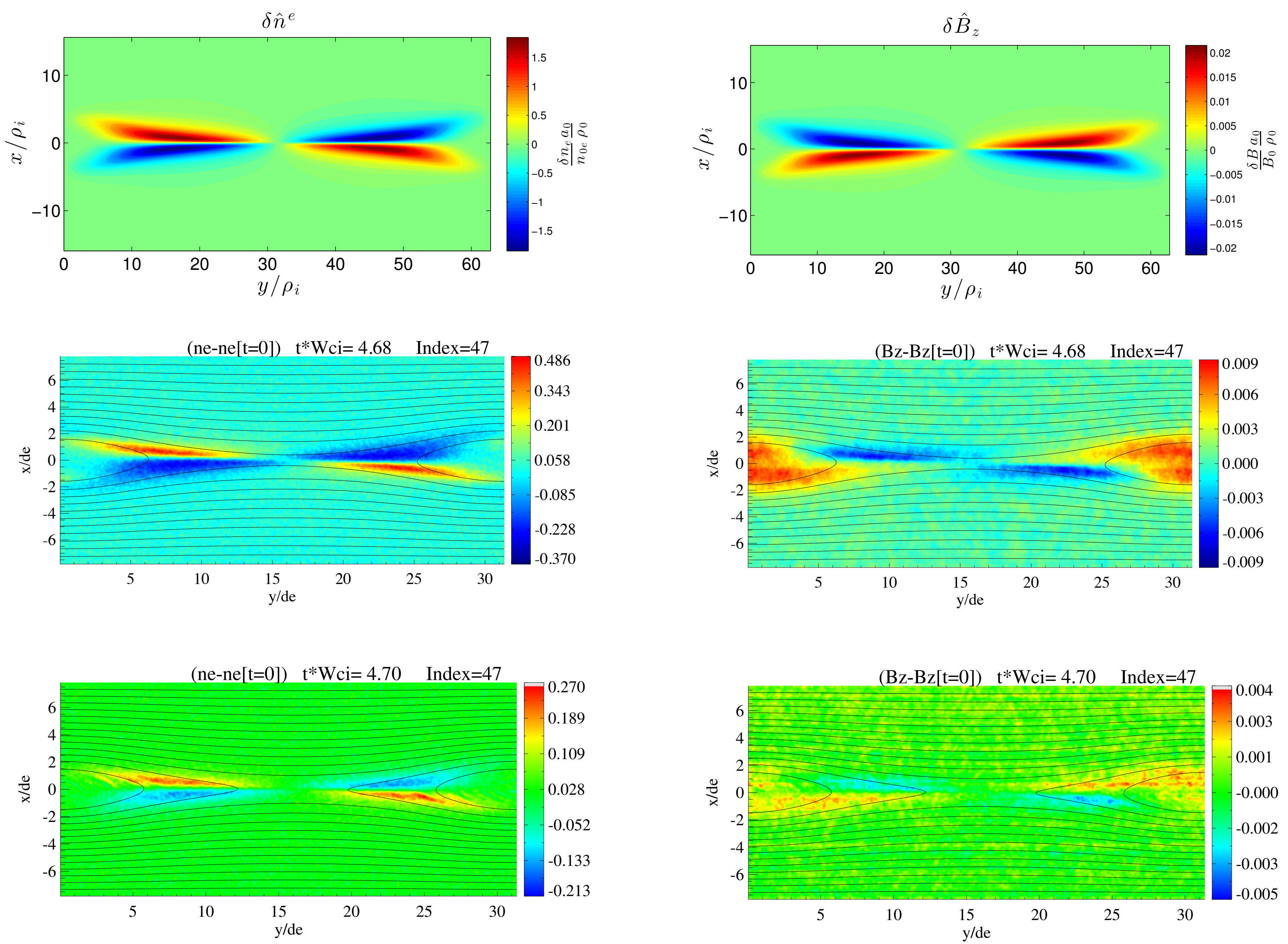

PIC Comparison δU_y^e and δU_y^i

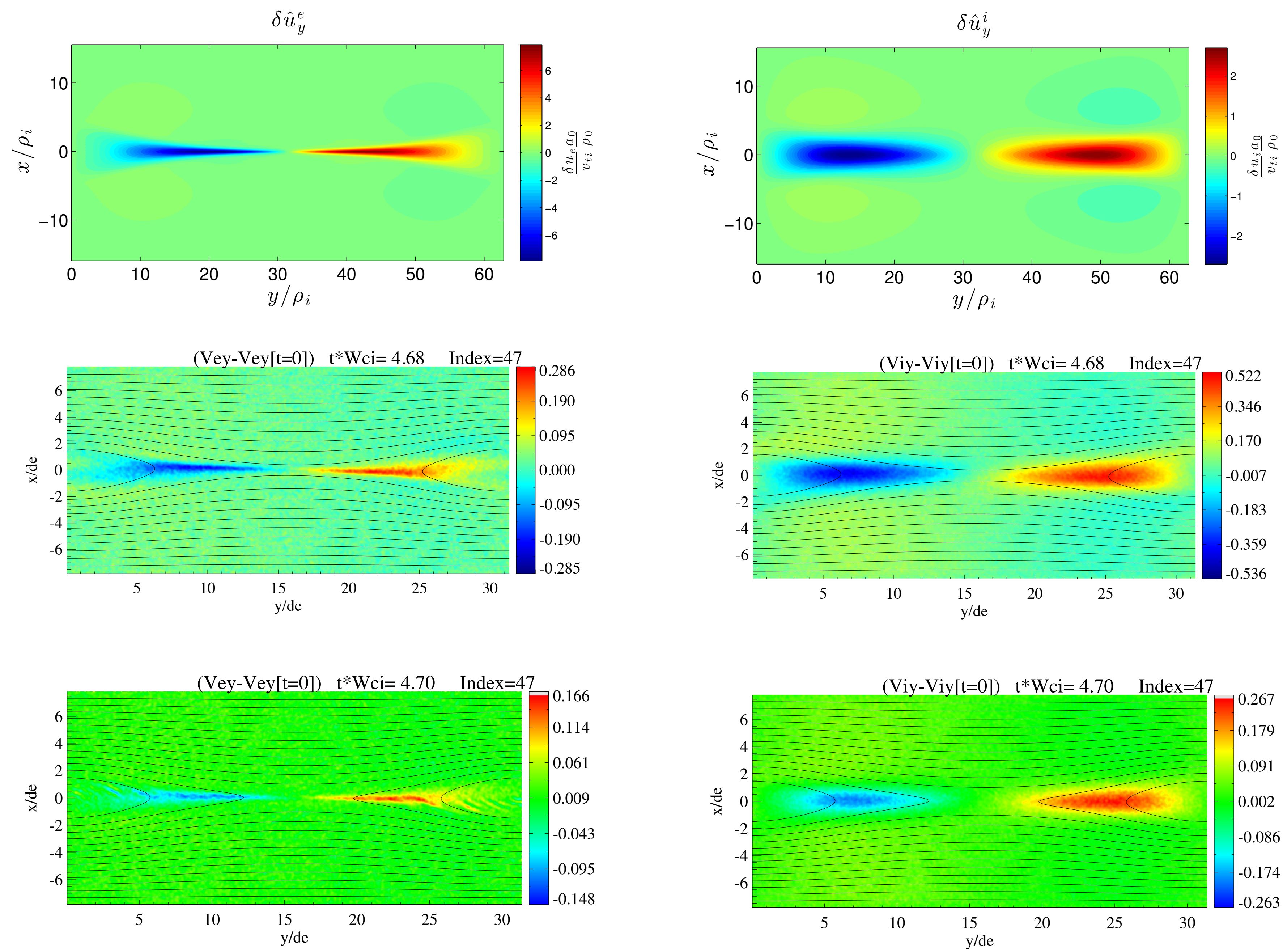

PIC Comparison Anisotropy

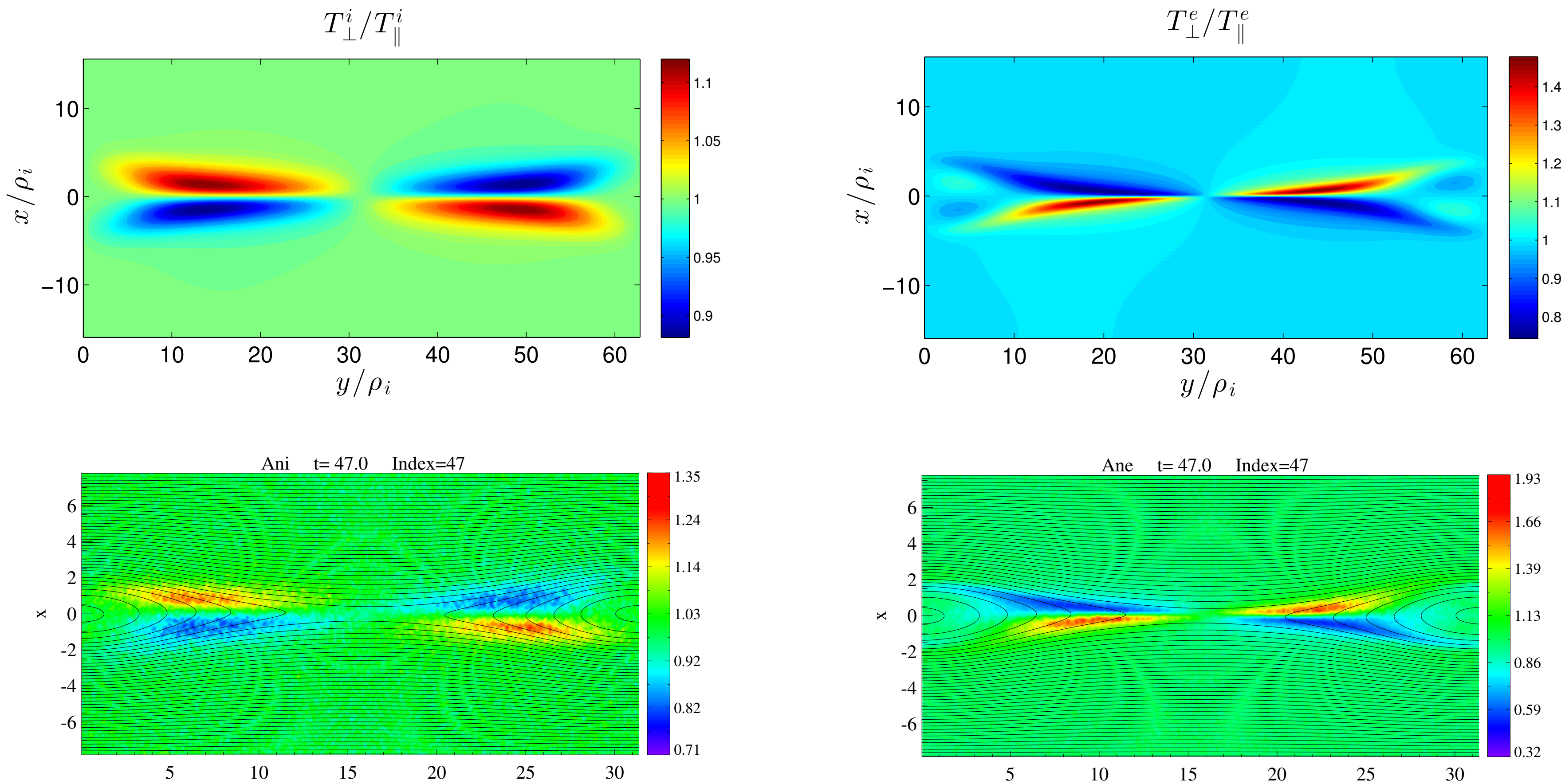

Summary

- Gyrokinetics can be a useful tool for the space and astrophysics communities
- Reproduce spectra in qualitative and quantitative agreement with solar wind data
- First evidence of critically balanced anisotropic cascade in a kinetic plasma
- Current sheets form as a natural consequence of wave-driven turbulence and correspond to locally enhanced heating rates
- Heating in current sheets can be due to reconnection, enhanced wave-particle interactions, or resistivity

Bibliography I

O. Alexandrova, J. Saur, C. Lacombe, A. Mangeney, J. Mitchell, S. J. Schwartz, and P. Robert. Universality of Solar-Wind Turbulent Spectrum from MHD to Electron Scales. *Phys. Rev. Lett.*, 103(16):165003–+, October 2009. doi: 10.1103/PhysRevLett.103.165003.

O. Alexandrova, C. Lacombe, A. Mangeney, R. Grappin, and M. Maksimovic. Solar Wind Turbulent Spectrum at Plasma Kinetic Scales. *Astrophys. J.*, 760:121, December 2012. doi: 10.1088/0004-637X/760/2/121.

S. D. Bale, J. C. Kasper, G. G. Howes, E. Quataert, C. Salem, and D. Sundkvist. Magnetic Fluctuation Power Near Proton Temperature Anisotropy Instability Thresholds in the Solar Wind. *Phys. Rev. Lett.*, 103(21):211101–+, November 2009. doi: 10.1103/PhysRevLett.103.211101.

J. Birn and E. R. Priest, editors. *Reconnection of Magnetic Fields*. Cambridge University Press, 2006.

A. Greco, W. H. Matthaeus, S. Servidio, P. Chuychai, and P. Dmitruk. Statistical Analysis of Discontinuities in Solar Wind ACE Data and Comparison with Intermittent MHD Turbulence. *Astrophys. J. Lett.*, 691: L111–L114, February 2009. doi: 10.1088/0004-637X/691/2/L111.

G. G. Howes, J. M. TenBarge, and W. Dorland. A weakened cascade model for turbulence in astrophysical plasmas. *Phys. Plasmas*, 18(10):102305, October 2011a. doi: 10.1063/1.3646400.

G. G. Howes, J. M. TenBarge, W. Dorland, E. Quataert, A. A. Schekochihin, R. Numata, and T. Tatsuno. Gyrokinetic Simulations of Solar Wind Turbulence from Ion to Electron Scales. *Phys. Rev. Lett.*, 107(3): 035004–+, July 2011b. doi: 10.1103/PhysRevLett.107.035004.

G. G. Howes, S. D. Bale, K. G. Klein, C. H. K. Chen, C. S. Salem, and J. M. TenBarge. The Slow-mode Nature of Compressible Wave Power in Solar Wind Turbulence. *Astrophys. J. Lett.*, 753:L19, July 2012. doi: 10.1088/2041-8205/753/1/L19.

K. H. Kiyani, S. C. Chapman, Y. V. Khotyaintsev, M. W. Dunlop, and F. Sahraoui. Global scale-invariant dissipation in collisionless plasma turbulence. *Physical Review Letters*, 103:075006, 2009.

R. J. Leamon, C. W. Smith, N. F. Ness, W. H. Matthaeus, and H. K. Wong. Observational constraints on the dynamics of the interplanetary magnetic field dissipation range. *J. Geophys. Res.*, 103:4775–4787, 1998.

K. T. Osman, W. H. Matthaeus, A. Greco, and S. Servidio. Evidence for Inhomogeneous Heating in the Solar Wind. *Astrophys. J. Lett.*, 727:L11, January 2011. doi: 10.1088/2041-8205/727/1/L11.

Bibliography II

E. N. Parker. *Spontaneous current sheets in magnetic fields : with applications to stellar x-rays*, volume 1. Oxford University Press, 1994.

J. J. Podesta and S. P. Gary. Magnetic Helicity Spectrum of Solar Wind Fluctuations as a Function of the Angle with Respect to the Local Mean Magnetic Field. *Astrophys. J.*, 734:15–+, June 2011. doi: 10.1088/0004-637X/734/1/15.

O. W. Roberts, X. Li, and B. Li. Kinetic plasma turbulence in the fast solar wind measured by Cluster. *ArXiv e-prints*, March 2013.

F. Sahraoui, M. L. Goldstein, P. Robert, and Y. V. Khotyaintsev. Evidence of a Cascade and Dissipation of Solar-Wind Turbulence at the Electron Gyroscale. *Physical Review Letters*, 102(23):231102–+, June 2009. doi: 10.1103/PhysRevLett.102.231102.

F. Sahraoui, M. L. Goldstein, G. Belmont, P. Canu, and L. Rezeau. Three Dimensional Anisotropic k Spectra of Turbulence at Subproton Scales in the Solar Wind. *Phys. Rev. Lett.*, 105(13):131101–+, September 2010. doi: 10.1103/PhysRevLett.105.131101.

J. M. TenBarge and G. G. Howes. Evidence of Critical Balance in Kinetic Alfven Wave Turbulence Simulations. *Phys. Plasmas*, 19(5):055901, 2012.

J. M. TenBarge, J. J. Podesta, K. G. Klein, and G. G. Howes. Interpreting Magnetic Variance Anisotropy Measurements in the Solar Wind. *Astrophys. J.*, 753:107, July 2012. doi: 10.1088/0004-637X/753/2/107.

J. M. TenBarge, G. G. Howes, and W. Dorland. Collisionless Dissipation at Electron Scales in the Solar Wind. *Astrophys. J.*, 2013a. submitted.

J. M. TenBarge, G. G. Howes, W. Dorland, and G. W. Hammett. An Oscillating Langevin Antenna for Driving Turbulence Simulations. *J. Comp. Phys.*, 2013b. in preparation.

B. J. Vasquez, V. I. Abramenko, D. K. Haggerty, and C. W. Smith. Numerous small magnetic field discontinuities of Bartels rotation 2286 and the potential role of Alfvénic turbulence. *J. Geophys. Res.*, 112:A11102, November 2007. doi: 10.1029/2007JA012504.